Dihydromyricetin Ameliorates Inflammation-induced Insulin Resistance via Phospholipase C-CaMKK-AMPK Signal Pathway

Lianjie Hou (houlianjie@gzhmu.edu.cn)
Guangdong Provincial Key Lab of Agro-Animal Genomics and Molecular Breeding, National Engineering Research Center for Breeding Swine Industry, College of Animal Science, South China Agricultural University, China

Fangyi Jiang
South China Agricultural University

Bo Huang
South China Agricultural University

Weijie Zheng
South China Agricultural University

Yufei Jiang
South China Agricultural University

Gengyuan Cai
South China Agricultural University

Dewu Liu
South China Agricultural University

Ching Yuan Hu
University of Hawai'i at Manoa

Chong Wang
South China Agricultural University

Research

Keywords: Insulin resistance, Dihydromyricetin, Inflammation, Obesity, Target protein

DOI: https://doi.org/10.21203/rs.3.rs-118119/v1

Abstract

Background: Metabolic syndrome is associated with obesity, inflammation, and insulin resistance. Patients with metabolic syndrome have a higher risk of turning into type II diabetes and cardiovascular disease. The metabolic syndrome has become an urgent public health problem. Insulin resistance in obesity is the common pathophysiological basis of metabolic syndrome. The insulin resistance is induced by the increasing levels of inflammatory factors during obesity. Therefore, developing a therapeutic strategy for preventing inflammation-induced insulin resistance has great significance for the treatment of metabolic syndrome. Dihydromyricetin, as a bioactive polyphenol, has been used for anti-inflammatory, anti-tumor, and improving insulin sensitivity. However, the target of DHM and the molecular mechanism of DHM in preventing inflammation-induced insulin resistance are still unclear.

Methods: In this study, we first confirmed the role of dihydromyricetin in inflammation-induced insulin resistance through ELISA, oral glucose tolerance test and glucose uptake test. Then, we demonstrated the pathway of dihydromyricetin ameliorated inflammation-induced insulin resistance by using signal pathway blockers, Ca2+ probes, and immunofluorescence. Finally, we clarified the target protein of dihydromyricetin by using drug affinity responsive target stability (DARTS) assay, qPCR, and western blotting.

Results: In this study, we first confirmed that dihydromyricetin ameliorated inflammation-induced insulin resistance in vivo and in vitro. Then, we demonstrated that dihydromyricetin ameliorated inflammation-induced insulin resistance by activating Ca2+-CaMKK-AMPK signal pathway. Finally, we clarified that dihydromyricetin activated Ca2+-CaMKK-AMPK signaling pathway by interacting with phospholipase C (PLC), its target protein.

Conclusions: Our results not only demonstrated that dihydromyricetin ameliorated inflammation-induced insulin resistance via the PLC-CaMKK-AMPK signal pathway but also discovered that the target protein of dihydromyricetin is PLC. Our results provided experimental data for the development of dihydromyricetin as a functional food additive and a new therapeutic strategy for treating or preventing insulin resistance and metabolic syndrome.

Introduction

With the changes in modern lifestyles, such as excessive energy intake, lack of regular exercise, and accelerated life rhythm, the incidence of metabolic syndrome-related diseases has increased year by year [1]. Metabolic syndrome is defined as a disorder of energy use and storage. This syndrome is characterized by central obesity, dyslipidemia, raised blood pressure, and high blood glucose levels [2]. Although the prevalence of metabolic syndrome varies globally based on race, age, and gender, the incidence rate is as high as 10–84%. Patients with metabolic syndrome have a higher risk of type II diabetes and cardiovascular disease [3]. Therefore, the metabolic syndrome has become an urgent public health problem.

Insulin resistance is the common pathophysiological basis of metabolic syndrome [4]. Insulin resistance is defined as a decrease in insulin sensitivity in the major insulin target organs such as adipose tissue, liver, and muscle. Insulin resistance is one of the significant characteristics of type II diabetes [5]. Studies have shown that insulin resistance has become a high-risk factor for chronic diseases such as type II diabetes, non-alcoholic fatty liver disease, cardiovascular disease, and even Alzheimer's disease [6]. Therefore, developing a therapeutic strategy for insulin resistance has great significance for the treatment of the metabolic syndrome.

The increase of pro-inflammatory cytokines, such as IL-1β, IL-6, TNFα, and MCP1, in adipose tissue during obesity, is the direct cause of insulin resistance [7]. Among the pro-inflammatory cytokines that induce insulin resistance, tumor necrosis factor α (TNFα) is the most representative one. Inflammatory cytokines impair insulin signaling and trigger insulin resistance. The main pathways of inflammation-induced insulin resistance include nuclear factor-kappa B (NF-κB) signaling pathway and c-Jun NH2-terminal kinase (JNK) signaling pathway [8]. NF-κB inhibits the activation of phosphatidylinositol 3-kinase (PI3K)-protein kinase B (AKT) signaling pathway by inhibiting phosphorylation of insulin receptor substrate (IRS), resulting in insulin resistance [9]. JNK inhibits the PI3K-AKT signaling pathway by down-regulating the expression and phosphorylation of the IRS, resulting in insulin resistance [10]. Therefore, inhibiting chronic inflammation is a promising therapeutic strategy to improve insulin resistance.

Dihydromyricetin (DHM), also known as ampelopsin, is the main bioactive polyphenol in rattan tea. Rattan tea has been used for anti-inflammatory in China and other Asian countries for several centuries [11]. DHM exerted its anti-inflammatory effect in rats through suppressing NF-kB signaling in macrophage [12]. DHM concentration-dependently increased the glucose uptake in insulin-resistant 3T3-L1 adipocytes induced by dexamethasone [13]. DHM also improved skeletal muscle insulin sensitivity by partially inducing autophagy via activation of the AMPK-PGC-1 alpha-Sirt3 signaling pathway [14]. DHM attenuated metabolic syndrome and improves insulin sensitivity by up-regulating Phosphorylation of IRS in db/db mice [15]. Currently, most DHM-related research reported that DHM functions depend on its activation of AMPK; but AMPK is not the direct target of DHM in cells, and the target of DHM in cells is still unclear. To our knowledge, there is no published paper demonstrated the DHM effect on inflammation-induced insulin resistance.

In this study, we used high fat diet (HFD) feeding to induce insulin resistance in vivo. Gavage DHM was used to determine DHM function in reducing the level of inflammation and inhibiting insulin resistance in obese mice. 3T3-L1 cells were treated with TNF-α as a model of inflammation-induced insulin resistance in vitro. We have elucidated the molecular mechanism of DHM for preventing inflammation-induced insulin resistance in 3T3-L1 using immunofluorescence, signal pathway blocking, and drug affinity responsive target stability (DARTS) assay. Our results provided not only experimental data for the development of DHM as a functional food additive but also offered a new therapeutic strategy for treating insulin resistance.

Materials And Methods

2.1. Animal experiment

Thirty-six 18-day-old specific pathogen free (SPF) healthy male C57B/L6 mice were purchased from the Animal Experiment Center of Guangdong Province. The mice were housed under a 12 h light and 12 h dark cycle (7 am and 7 pm, 25 °C and 70 ~ 80% humidity). The mice were divided into three groups (n = 12) randomly: Chow diet + PBS gavage (control), the HFD + PBS gavage (HFD), and the HFD + DHM gavage (DHM). Two-hundred μL of DHM (200 mg/kg body weight) was administered orally by gavage to the DHM group daily, while the control group and the HFD group were administered the same volume of PBS each day. The BW and feed intake of the mice were recorded every week. At week 10, we analyzed the body composition of mice. At week 11, we tested insulin sensitivity in mice using an oral glucose tolerance test. At week 12, the mice were euthanized to collect serum, inguinal white adipose tissue (iWAT), epididymis white adipose tissue (eWAT), and other tissues for further analysis. All experiments were conducted following “The Instructive Notions with Respect to Caring for Laboratory Animals” issued by the Ministry of Science and Technology of the People’s Republic of China. All experimental protocols and methods were approved by the College of Animal Science, South China Agricultural University.

2.2. Oral glucose tolerance test

After fasting for about 12 hours, the blood glucose of the mice was measured by ACCU-CHEK MOBILE (Roche, Mannheim, Germany). Then the mice were given oral administration of glucose (1.0 g/kg) solution. After 30, 60, 90, 120, and 180 min, blood samples were collected via the tail vein for the measurement of blood glucose levels.

2.3. Hematoxylin-eosin staining (H&E)

The mice adipose tissue was fixed in 4% formaldehyde (DaMao, Tianjin, China) at room temperature for 48 h. The method used for the H&E staining has been described previously [16].

2.4. Body composition analysis

Fat mass, lean mass, and body composition were determined using a nuclear magnetic resonance system according to the manufacturer’s instruction (Body Composition Analyzer MiniQMR23-060H-I, Niumag Corporation, Shanghai, China).

2.5. 3T3-L1 culture and inflammatory induce 3T3-L1 insulin resistance

The 3T3-L1 cell line used in this study was purchased from American Type Culture Collection (ATCC, VA, USA). 3T3-L1 were cultured in DMEM/HIGH GLUCOSE (Hyclone, PA, USA) with 10% Fetal Bovine Serum (Gibco, NY, USA). 3T3-L1 cells were seeded in 24-well plates (4×10^5 /cm^2). After 24 h, we treated the 3T3-L1 with TNFα (MedChemExpress, Monmouth Junction, USA) at the concentration of 1 ng/mL for 5 days to induce 3T3-L1 insulin resistance. We treated 3T3-L1 cells with TNFα and DHM (1 μM, Sigma Chemical Inc., Louis, MO, USA) for 5 days to demonstrate DHM ameliorated inflammation-induced insulin resistance. We treated 3T3-L1 cells with TNFα, DHM, and Compound C (5 μM, MedChemExpress,

Monmouth Junction, USA) for 5 days to demonstrate DHM ameliorated inflammation-induced insulin resistance through AMPK. We treated 3T3-L1 cells with TNFα, DHM, and STO-609 (10 ng/mL, MedChemExpress, Monmouth Junction, USA) for 5 days to demonstrate DHM ameliorated inflammation-induced insulin resistance through CaMKK. We treated 3T3-L1 cells with TNFα, DHM, and U73122 (1 μM, MedChemExpress, Monmouth Junction, USA) for 5 days to demonstrate DHM ameliorated inflammation-induced insulin resistance through the PLC-IP3 receptor pathway.

2.6. Glucose uptake assay

Five days after treatments, the glucose uptake was assayed by 2-NBDG (MedChemExpress, Monmouth Junction, USA) according to the manufacturer's protocol. 3T3-L1 were incubated with or without media containing 10 nM insulin (Sigma Chemical Inc., Louis, MO, USA) for 10 minutes. The media was changed to low-glucose DMEM containing 150 μg/mL 2-NBDG for 60 minutes at 37 °C. The medium was removed, and cells were washed 5 times with PBS. Nikon Eclipse Ti-s microscopy (Nikon, Tokyo, Japan) was used to observe fluorescence. Fluorescent data were acquired at excitation and emission wavelengths of 490 and intensity at 525 nm.

2.7. Methyl Thiazolyl diphenyl-tetrazolium bromide (MTT)

3T3-L1 cells were seeded in 96-well plates at a density of 3×10^4 / cm^2. After 12 h culture, 15 μL of treatments (TNF or DHM) with different concentrations were added to the cells for another 24 h of incubation. MTT was performed according to the manufacturer's protocol (M1020-500T, Solarbio, Beijing, China).

2.8. Calcium (Ca^{2+}) imaging

Ca^{2+} was measured by a Ca^{2+} fluorescent probe fluo-4-AM kit following the manufacturer's instructions. 3T3-L1 cells were incubated with ryanodine (100 nM, MedChemExpress, Monmouth Junction, USA) or U73122 (1 μM, MedChemExpress, Monmouth Junction, USA) for 1 h to block the endoplasmic reticulum Ca^{2+} channel. Then the cells were washed 3 times with Hank's Balanced Salt Solution and incubated with 10 μM fluo-4-AM at 37 °C for 1 h. After incubation, cells were then rewashed 3 times. Nikon Eclipse Ti-s microscopy (Nikon, Tokyo, Japan) was used to observe fluorescence. Fluorescent data were acquired after excitation at 490 nm and intensity at 525 nm.

2.9. RNA Extraction and PCR Analysis

Methods used for the RNA extraction and PCR analysis have been described previously [17]. The relative expression of mRNAs was normalized with β-actin levels using the $2^{-\Delta\Delta Ct}$ method. $2^{-\Delta\Delta Ct}$ is defined as the ratio of the relative mRNA level between the experimental group and the control group. Primers were designed using Primer Premier 5 based on sequences of mice genes obtained from NCBI. All the primers used in this study are shown in Table 1.

Table 1
The primers used in this study

Gene name	Forward primer sequence (5’-3’)	Reversed primer sequence (5’-3’)
β-actin	TCGTACCACTGGCATTGTGAT	CGAAGTCTAGGGCAACATAG
NF-κB	ATGCCAGTGAGAATGTATGC	ACGCAGGAGACGGAAGAAT
IRS-1	ATGTCGCCAGTGGGAGATT	CTTCGGCAGTTGCGGTATA
PI3K	GACCAATACTTGATGTGGCTG	TCCCTCGCAATAGGTTCTCC
AKT	GCCCGCTTCTATGGTGC	CTTCTCGTGGTCCTGGTTGTA
JNK	CCAGCACCCATACATCAAC	TTCCTCCAAATCCATTACCTCC
GLUT4	AGTATGTTGCGGATGCTATGG	CTGCTCTAAAAGGTAAGGTGT

2.10. Western Blot Analysis

The method used for the Western blot analysis has been described previously [18]. Band intensities were quantified by Image J software. The antibodies and their dilutions used in this study are listed in Table 2.

Table 2
The details of antibodies used in this study

Primary antibody	Clone	Company	Catalog No.	Dilution
PLC	Polyclonal	Abcam	Ab41433	1:2000
CaMKK	Polyclonal	Abbkine	ABP53531	1:1000
p-CaMKK	Polyclonal	Affinit	AF4487	1:1000
LKB1	Polyclonal	Bioss	bs-3948R	1:2000
AMPK	Polyclonal	Abbkine	ABP50650	1:1000
p-AMPK	Polyclonal	Abbkine	ABP50452	1:1000
JNK	Polyclonal	ZEN BIO	380556	1:2000
NF-κB	Polyclonal	Bioss	bsm-33117M	1:5000
p-NF-κB	Polyclonal	Bioss	bs-3485R	1:500
IRS-1	Polyclonal	Abcam	341420	1:1000
p-IRS-1	Polyclonal	Abcam	Ab3690	1:2000
AKT	Monoclonal	CST	# 9272S	1:2000
p-AKT	Monoclonal	CST	# 4058S	1:2000
PI3K	Polyclonal	ZEN BIO	385369	1:1000
p-PI3K	Polyclonal	ZEN BIO	530854	1:1000
GLUT4	Polyclonal	Abcam	ab109313	1:2000
β-actin	Monoclonal	Bioworld	BS6007M	1: 5000
Secondary antibody	Conjugate Used	Company	Catalog No.	Dilution
Goat Anti-rabbit IgG	HRP	Bioss	bs-0295G	1:5000
Goat anti-Mouse IgG	HRP	Bioworld	BS12478	1:50000

2.11. Drug affinity responsive target stability (DARTS) assay

DARTS experiments for identifying the targets of DHM were performed as previously reported [19]. In brief, 3T3-L1 cells were lysed and treated with DHM (10 nM or 1 μM) for 1 hour at room temperature. Then the mixture was digested with 0.01% protease for 30 min at room temperature. The digestion was stopped by directly add 5 × SDS-PAGE loading buffer and inactivation by boiling 5 min. Protein samples were separated with 8%-15% SDS-polyacrylamide gels and analyzed by Coomassie blue staining and western blotting.

2.12. Statistical analysis

All data are expressed as the mean ± standard error of the mean (SEM) of three independent experiments. Our data is a normal distribution, and the homogeneity of data between each treatment group is equal under the SPSS analysis. In Fig. 3D and Fig. 6E the unpaired Student's t-test was used for p-value calculations, where * is $p < 0.05$; and ** is $p < 0.01$. The data of the remaining results are in a normal distribution, and homogeneity of data between each treatment group is equal by SPSS analysis. Significant differences between treatment groups were determined by one-way ANOVA with the LSD test (SPSS v18.0, IBM Knowledge Center, Chicago, IL, USA). Bars with different letters indicate they are significantly different ($p < 0.05$).

Results

3.1. DHM reduced fat accumulation and inflammation in HFD-induced obese mice

Compared with the HFD group, HFD not only increased energy intake and body weight gain in mice (Figures 1A and 1B), HFD also increased fat mass (Figures 1C), indicating the HFD-induced obese mice model were constructed successfully. Compared with the HFD group, DHM did not affect energy intake and body weight gain (Figures 1A and 1B), but HFD prevented the increase of fat mass caused by HFD (Figures 1C). Both percentages of inguinal white adipose tissue (iWAT) weight/body weight and epididymis white adipose tissue (eWAT) weight/body weight were increased in HFD-induced obese mice compared with the control group (Figure 1D and 1E). DHM reversed the HFD-induced eWAT and iWAT hypertrophy (Figure 1D and 1E). We found HFD increased the diameter of adipocytes in iWAT and eWAT, while DHM inhibited the hypertrophy of adipocytes caused by HFD, based on the H&E results (Figure 1F). For the energy metabolism-related parameters, HFD increased the levels of glucose, insulin, total triglycerides, total cholesterol, and free fatty acids in serum. DHM alleviated the increase of energy metabolism-related parameters in serum caused by HFD (Figure 1G). Since obesity is always accompanied by low-level inflammation, we also measured the level of the inflammatory cytokines in the serum. HFD induced a higher level of IL-1β, IL-6, TNFα, and MCP1 in obese mice, as measured by ELISA. DHM reduced the increase in the HFD-induced inflammatory cytokines in the serum (Figure 1H). These results indicate that DHM reduced fat accumulation and inflammation in HFD-induced obese mice.

3.2. DHM ameliorated insulin resistance induced by inflammation in HFD mice

To investigate whether DHM ameliorated insulin resistance induced by inflammation, we measured the level of inflammatory cytokines in adipose tissue and insulin sensitivity in mice. ELISA results showed that HFD caused an increase in inflammatory cytokines IL-1β, IL-6, TNFα, and MCP1 in adipose tissue, while DHM reduced the level of adipose tissue inflammatory cytokines induced by HFD (Figure 2A). Through the oral glucose tolerance test, we found that the glucose clearance ability was decreased in the HFD-induced obese mice, while DHM enhanced the ability of glucose clearance in the HFD-fed mice. qPCR and western blot results also showed that phosphorylation of AMPK, an adipose tissue energy metabolism sensor, was inhibited in HFD-induced obese mice. HFD-induced obesity activated the

expression of NF-κB and JNK. NF-κB and JNK, they, in turn, inhibited the phosphorylation of IRS-1, PI3K, AKT, indicating that HFD induced insulin resistance. The insulin resistance, subsequently, inhibited the expression of GLUT4, a transporter for glucose uptake (Figures 2H and 2I). However, DHM increased the phosphorylation of AMPK and inhibited the activation of NF-κB and JNK induced by HFD. DHM reversed the inhibition of phosphorylation on IRS-1, AKT, and PI3K induced by HFD, and finally increased GLUT4 expression. These results indicate that DHM ameliorated inflammatory-induced insulin resistance in HFD mice.

3.3. TNFα induced inflammatory response and insulin resistance in 3T3-L1 cells

We constructed a cellular model of TNFα-induced insulin resistance in 3T3-L1 cells to establish the mechanism of DHM in relieving HFD-induced inflammation and insulin resistance. TNFα, less than 50 ng/mL, did not damage cell viability based on the result of MTT assay (Figure 3A). To simulate the low-level inflammatory response during obesity, we selected the TNFα concentration of 1 ng/mL for five days in subsequent experiments. After five days of TNFα treatment, insulin stimulation did not increase glucose uptake in 3T3-L1 cells, and the cells developed an insulin resistance phenotype (Figure 3B and 3C). qPCR and western blot results also showed that phosphorylation of AMPK was inhibited after TNFα treatment. TNFα treatment activated the expression of NF-κB and JNK. NF-κB and JNK, they, in turn, inhibited the phosphorylation of IRS-1, PI3K, and AKT, indicating that TNFα induced insulin resistance. The insulin resistance, subsequently, inhibited the expression of GLUT4 (Figures 3D and 3E). Thus, these results suggest that TNFα activated the inflammatory response and induced insulin resistance.

3.4. DHM ameliorated the inflammatory-induced insulin resistance

We then investigated whether DHM prevented insulin resistance induced by the inflammatory response. DHM, less than 30 μM, did not damage cell viability based on MTT assay (Figure 4A). Insulin stimulation did not increase glucose uptake in 3T3-L1 cells after TNFα treatment (Figure 4B and 4C), while DHM prevented the TNFα-induced insulin resistance (Figure 4B and 4C). Compared with TNFα treatment, co-treatment with TNFα and DHM, the phosphorylation of AMPK was activated, and the expression of NF-κB and JNK was inhibited, as shown by the qPCR and WB results (Figure 4D and 4E). Compared with TNFα treatment, DHM increased the phosphorylation of IRS-1, PI3K, and AKT, indicating that DHM ameliorated the TNFα-induced insulin resistance (Figure 4D and 4E). The improvement of insulin sensitivity, subsequently, increased the expression of GLUT4 (Figure 4D and 4E). Thus, the above results indicate that DHM ameliorated insulin resistance induced by inflammation.

3.5. DHM ameliorated inflammation-induced insulin resistance through AMPK

We blocked AMPK activity using Compound C to investigate whether DHM exerted its anti-insulin resistance function through AMPK in 3T3-L1 cells. The ability of DHM to improve TNFα-induced insulin resistance was blocked by inhibiting AMPK, as shown by the glucose uptake assay (Figure 5A and 5B). When Compound C blocked AMPK activity, the activation effect of DHM on phosphorylation of AMPK, IRS-1, PI3K, and AKT, and mTOR disappeared (Figure 6C), and the promotion effect of DHM on the

expression of GLUT4 also disappeared (Figure 6C and 6D). Blocked AMPK, the DHM inhibitory effect on the expression of NF-κB and JNK was eliminated (Figure 6C and 6D). These results indicate that DHM ameliorated inflammation-induced insulin resistance in 3T3-L1 cells through AMPK.

3.6. DHM ameliorated inflammation-induced insulin resistance through CaMKK-AMPK instead of LKB1-AMPK pathway

We blocked the AMPK upstream factors CaMKK and LKB1 to investigate the pathway DHM used to activate AMPK. When STO-609 blocked CaMKK activity, the ability of DHM to improve TNFα-induced insulin resistance disappeared, as shown by the glucose uptake assay (Figure 6A and 6B). When STO-609 blocked CaMKK activity, the activation effect of DHM on phosphorylation of CaMKK, AMPK, IRS, PI3K, and AKT disappeared (Figure 6C and 6D) and the promotion effect of DHM on the expression of GLUT4 also disappeared (Figure 6C and 6D). Blocked CaMKK also caused DHM to lose its inhibitory effect on the expression of NF-κB and JNK (Figure 6C and 6D). We then interfered with LKB1 expression using siRNA (Figures 6E and 6F). LKB1 interference did not affect the activation of AMPK by DHM (Figure 6F). LKB1 interference did not affect the improvement of DHM on TNFα-induced insulin resistance, as shown by the glucose uptake assay (Figure 6G and 6H). These results indicate that DHM ameliorated inflammation-induced insulin resistance in 3T3-L1 cells through CaMKK-AMPK instead of the LKB1-AMPK pathway.

3.7. DHM activated CaMKK by increasing intracellular Ca^{2+} concentration through PLC-IP3 receptor pathway

CaMKK was regulated by cellular Ca^{2+}, so we investigated whether DHM activated cellular Ca^{2+} signal. DHM treatment activated intracellular Ca^{2+} signal, as shown by the Ca^{2+} probe test. When Ca^{2+} was removed from the extracellular medium, DHM still increased intracellular Ca^{2+} level (Figure 7A). After the cellular Ca^{2+} was cleared by the intracellular Ca^{2+} chelating agent BATAP-AM, the activation effect of DHM on intracellular Ca^{2+} was eliminated, indicating that DHM activation on intracellular Ca^{2+} was dependent on intracellular Ca^{2+} storage (Figure 7B). After cellular Ca^{2+} was cleared, DHM could no longer activate CaMKK, as shown by the WB results (Figure 7C). Endoplasmic reticulum was the major organelle for Ca^{2+} release and recovery in cells. We used U73122, a phospholipase C (PLC) inhibitor, to block the endoplasmic reticulum Ca^{2+} channel IP3 receptor by preventing phospholipid phosphatidylinositol 4, 5-diphosphate (PIP2) from degrading into inositol 1, 4, 5-triphosphate (IP3). We also used ryanodine to block the Ca^{2+} channel ryanodine receptor. Blocking the ryanodine receptor did not affect cellular activation of intracellular Ca^{2+} signal induced by DHM (Figure 7D). After the PLC-IP3 receptor pathway blocked, the DHM function on activating the intracellular Ca^{2+} signal disappeared (Figure 7D). After blocking the PLC-IP3 receptor pathway, DHM failed to activate CaMKK, as shown by the WB results (Figure 7E). These results indicate that DHM activated CaMKK by increasing intracellular Ca^{2+} concentration through the PLC-IP3 receptor pathway.

3.8. DHM ameliorated inflammatory-induced insulin resistance through interaction with PLC

We verified the interaction of DHM and PLC by drug affinity responsive target stability (DARTS) assay to investigate the pathway DHM used to activate the PLC-IP3 receptor pathway. From the DARTS results, we found a brighter band at the position of about 50 KD SDS-PAGE gel in the DHM treatment group, suggesting that DHM might interact with the PLC (Figure 8A). At the same time, we also detected the DARTS product through WB. DHM promoted the stability of PLC protein, as shown by the WB results, indicating that DHM interacted with PLC protein (Figure 8B). When U73122 blocked the PLC-IP3 receptor pathway, the activation effect of DHM on phosphorylation of CaMKK, AMPK, IRS-1, PI3K, and AKT disappeared (Figure 8C), and the promotion effect of DHM on the expression of GLUT4 also disappeared (Figure 8C and 8D). Blocked PLC-IP3 receptor pathway also caused DHM to lose its inhibitory effect on the expression of JNK and NF-κB (Figure 8C and 8D). When U73122 blocked the PLC-IP3 receptor pathway, the ability of DHM to improve TNFα-induced insulin resistance disappeared, as shown by the glucose uptake assay (Figure 8E and 8F). These results indicate that DHM ameliorated inflammatory-induced insulin resistance through interaction with the PLC.

Discussion

Increasing incidence of metabolic syndrome-related diseases such as obesity, diabetes, and cardiovascular diseases has become a global health problem. Insulin resistance is the common pathophysiology basis of metabolic syndrome. All metabolic syndrome patients have insulin resistance in different degrees. Therefore, therapeutic strategies for metabolic syndrome need to ameliorate insulin resistance. In this study, we found that DHM activated the Ca^{2+}-CaMKK-AMPK signal pathway by binding to the PLC. Activation of AMPK ameliorated adipocytes insulin resistance by blocking the inflammation factor-induced inflammatory response. Our study not only clarified the molecular mechanism of DHM in inflammation-induced insulin resistance but also discovered the target of DHM in this process. This study offers a new therapeutic strategy for patients with metabolic syndrome.

The increasing incidence of insulin resistance is inextricably related to the increase in the global obese population [20]. A recent report showed that 2.1 billion people, about 30% of the world population were either overweight or obese. During the process of obesity, the proliferation and hypertrophy of adipocytes triggered hypoxic stress, causing the secretion of inflammatory cytokines [21]. Our results showed that levels of serum and adipose tissue inflammatory cytokines were increased in HFD-induced obese mice.

The inflammatory cytokines secreted by adipose tissue activated NF-κB and JNK signal pathways in insulin-sensitive organs like adipose tissue, skeletal muscle, and liver [22–24]. The activation of NF-κB and JNK inhibited the phosphorylation of IRS-1, and, in turn, blocked the PI3K/AKT activation [25]. Results from our in vivo experiments showed that the level of the inflammatory cytokines was increased in adipose tissue, the inflammatory cytokines induced the NF-κB and JNK-1 activation and insulin resistance in mice. Results from our in vitro experiments also showed that TNFα induced the NF-κB and JNK-1 activation and insulin resistance in 3T3-L1 cells.

AMPK is not only an important regulator in cellular energy metabolism but also plays an essential role in many physiological processes such as tumor growth, inflammation, and enhanced insulin sensitivity [26]. The pharmacological function of DHM to activate AMPK has been demonstrated in various physiological processes. DHM improved skeletal muscle insulin sensitivity partially through inducing autophagy by activating the AMPK-PGC-1α-Sirt signaling pathway [27]. DHM protected rats from developing Alzheimer's disease via the up-regulation of the AMPK-SIRT1 pathway to inhibit inflammation-induced apoptosis of hippocampal cells and ameliorate cognitive function [28]. We demonstrated that DHM activated AMPK *in vivo* and *in vitro*, and we also demonstrated that the function of DHM in ameliorating insulin resistance depended on its activation effect on AMPK *in vitro.*

AMPK blocked the inflammatory response by inhibiting the NF-κB signaling pathway. AMPK activation blocked the phosphorylation of IKK and NF-κB directly [29]. AMPK also activated SIRT1, then P65, the subunit of NF-κB, was deacetylated by SIRT1. Thus, the transcriptional activity of NF-κB was also inhibited [30]. In this study, we found that DHM blocked NF-κB phosphorylation to ameliorate insulin resistance through AMPK *in vivo* and *in vitro*.

To our knowledge, most DHM-related research reported that DHM functions depend on its activation of AMPK [11; 31]; but AMPK is not the direct target of DHM in cells, and the target of DHM in cells has not been identified. Two predominant upstream kinases are known to activate AMPK: LKB1 and CaMKK [32]. Cynandione A, a Cynanchum wilfordii extract, inhibited lipogenesis by activating the LKB1-AMPK pathway in HepG2 cells [33]. Apigenin, a natural flavonoid, induced autophagy in human keratinocytes via up-regulating CaMKK-AMPK [34]. To investigate the pathway DHM used to activate AMPK, we blocked the AMPK upstream factors LKB1 and CaMKK. Results from our *in vitro* experiment showed that DHM ameliorated inflammation-induced insulin resistance through CaMKK-AMPK instead of the LKB1-AMPK pathway.

As far as we know, there is no published report on how DHM activates CaMKK. Triptolide, an extract from the Chinese herb thunder god vine, increased intracellular Ca^{2+} by stimulating the endoplasmic reticulum stress. The triptolide induced autophagy in human prostate cancer cells by activating the Ca^{2+}-CaMKK-AMPK signaling pathway [35]. Brosimone I, a flavonoid from Artocarpus heterophyllus, increased intracellular Ca^{2+} by stimulating the endoplasmic reticulum stress. Brosimone I induced cell cycle arrest and apoptosis via the activation of the Ca^{2+}-CaMKK-AMPK signaling pathway [36]. These reports showed that plant extracts could activate the CaMKK-AMPK signaling pathway through Ca^{2+}. In this study, we found that the DHM activated CaMKK-AMPK signaling pathway is dependent on Ca^{2+}. Dandelion root extract (10–400 μg/mL) dose-dependently increased intracellular Ca^{2+} level in the presence of external Ca^{2+}. The effect of dandelion root extract-induced Ca^{2+} increase was inhibited in the absence of extracellular Ca^{2+} [37]. However, in our study, DHM activated intracellular Ca^{2+} signals regardless of the presence or absence of extracellular Ca^{2+}. The endoplasmic reticulum is the main storage organelle for Ca^{2+} in cells. The ryanodine receptor and IP3 receptor are the main channels for calcium release from the endoplasmic reticulum and play a central role in cellular Ca^{2+} signal transduction [38]. In this study, we

discovered that by blocking the PLC-IP3 receptor pathway, the DHM's ability to activate Ca^{2+} and CaMKK disappeared, but blocking the ryanodine receptor had no effect on preventing the activation of Ca^{2+}-CaMKK induced by DHM.

The identification of target protein for small molecules is critical for drug discovery and chemical metabolomics [39]. DARTS is a quick and straightforward approach to identify potential target protein of small molecules. The mechanism of DARTS is that the interaction of small molecule and target protein resists proteolysis. The most significant advantage of this method is it allows the use of the small native molecule without any modification, such as the incorporation of biotin, photo-affinity labels, or radioisotope [40; 41]. In this study, we used DARTS to identify potential binding targets of DHM and used DARTS-Western blotting to test and validate the potential DHM target. Our results showed that DHM interacted with PLC to activate the Ca^{2+}-CaMKK-AMPK signal pathway.

In conclusion, our results not only showed that DHM ameliorated inflammation-induced insulin resistance but also demonstrated that DHM activated the Ca^{2+}-CaMKK-AMPK signal pathway through interacting with its target protein phospholipase C (Fig. 9). Our results provided experimental data for the development of DHM as a functional food additive and new therapeutic strategies for treating or preventing insulin resistance.

Declarations

Ethics approval and consent to participate

All experiments were conducted following "The Instructive Notions with Respect to Caring for Laboratory Animals" issued by the Ministry of Science and Technology of the People's Republic of China. All experimental protocols and methods were approved by the College of Animal Science, South China Agricultural University.

Consent for publication

Not applicable.

Availability of data and materials

The data and materials supporting the conclusions are included within the article and its supplementary information files.

Competing interests

The authors declare no conflict of interest.

Funding

This work was supported by the South China Agricultural University Major Project for International Science and Technology Cooperation Cultivation (2019SCAUGH01), the Guangdong Provincial Key Area Research and Development Program (2018B020203002), the China Postdoctoral Science Foundation (2018M640789), and the Common Technical Innovation Team on Agricultural Seed Industry of Guangdong Province.

Authors' contributions

Lianjie Hou: Formal analysis, Investigation, Validation, Visualization, Writing-original draft, Writing-review & editing. Meiying Xie: Investigation, Validation. Fangyi Jiang: Formal analysis, Investigation, Visualization. Bo Huang: Formal analysis, Investigation. Weijie Zheng: Formal analysis, Resources. Yufei Jiang: Formal analysis, Resources. Dewu Liu: Funding acquisition. Gengyuan Cai: Funding acquisition, Writing-review & editing. Ching Yuan Hu: Conceptualization, Formal analysis, Investigation, Validation, Visualization, Writing-review & editing. Chong Wang: Funding acquisition, Investigation, Project Administration, Resources, Supervision, Validation, Visualization, Writing-review & editing.

Acknowledgements

No.

References

[1] Despres, J. P., Lemieux, I., 2006. Abdominal obesity and metabolic syndrome. Nature 444(7121):881-887.

[2] Grundy, S. M., 2016. Metabolic syndrome update. Trends in Cardiovascular Medicine 26(4):364-373.

[3] Aballay, L. R., Eynard, A. R., Diaz, M. D., Navarro, A., Munoz, S. E., 2013. Overweight and obesity: a review of their relationship to metabolic syndrome, cardiovascular disease, and cancer in South America. Nutrition Reviews 71(3):168-179.

[4] Alwahsh, S. M., Dwyer, B. J., Forbes, S., van Thiel, D. H., Lewis, P. J. S., Ramadori, G., 2017. Insulin Production and Resistance in Different Models of Diet-Induced Obesity and Metabolic Syndrome. International Journal of Molecular Sciences 18(2).

[5] Czech, M. P., 2017. Insulin action and resistance in obesity and type 2 diabetes. Nature Medicine 23(7):804-814.

[6] Patel, T. P., Rawal, K., Bagchi, A. K., Akolkar, G., Bernardes, N., Dias, D. D., et al., 2016. Insulin resistance: an additional risk factor in the pathogenesis of cardiovascular disease in type 2 diabetes. Heart Failure Reviews 21(1):11-23.

[7] Esser, N., Legrand-Poels, S., Piette, J., Scheen, A. J., Paquot, N., 2014. Inflammation as a link between obesity, metabolic syndrome and type 2 diabetes. Diabetes Research and Clinical Practice 105(2):141-150.

[8] Bastard, J. P., Maachi, M., Lagathu, C., Kim, M. J., Caron, M., Vidal, H., et al., 2006. Recent advances in the relationship between obesity, inflammation, and insulin resistance. European Cytokine Network 17(1):4-12.

[9] Guo, C., Huang, T., Chen, A., Chen, X., Wang, L., Shen, F., et al., 2016. Glucagon-like peptide 1 improves insulin resistance in vitro through anti-inflammation of macrophages. Brazilian Journal of Medical and Biological Research 49(12).

[10] Solinas, G., Vilcu, C., Neels, J. G., Bandyopadhyay, G. K., Luo, J. L., Naugler, W., et al., 2007. JNK1 in hematopoietically derived cells contributes to diet-induced inflammation and insulin resistance without affecting obesity. Cell metabolism 6(5):386-397.

[11] H, Tong, X, Zhang, L, Tan, R, Jin, S, Huang, X, Li, 2020. Multitarget and promising role of dihydromyricetin in the treatment of metabolic diseases. European journal of pharmacology 870:172888.

[12] TT, Liu, Y, Zeng, K, Tang, X, Chen, W, Zhang, XL, Xu, 2017. Dihydromyricetin ameliorates atherosclerosis in LDL receptor deficient mice. Atherosclerosis 262:39-50.

[13] Wan, Xing-Yi, Gao, Li-hui, Feng, Guo-hua, Zhang, Yuan, Liu, Xu, Li, Ling, 2014. Effects of dihydromyricetin on insulin resistance in 3T3-L1 adipocytes and its mechanism. Chinese Pharmacological Bulletin 30(11):1580-1585.

[14] Shi, Linying, Zhang, Ting, Zhou, Yong, Zeng, Xianglong, Ran, Li, Zhang, Qianyong, et al., 2015. Dihydromyricetin improves skeletal muscle insulin sensitivity by inducing autophagy via the AMPK-PGC-1 alpha-Sirt3 signaling pathway. Endocrine 50(2):378-389.

[15] He, Jidong, Zhang, Junpeng, Dong, Lijuan, Dang, Xuefeng, Wang, Li, Cheng, Long, et al., 2019. Dihydromyricetin Attenuates Metabolic Syndrome And Improves Insulin Sensitivity By Upregulating Insulin Receptor Substrate-1 (Y612) Tyrosine Phosphorylation In db/db Mice. Diabetes Metabolic Syndrome and Obesity-Targets and Therapy 12:2237-2249.

[16] Hochstim, C. J., Choi, J. Y., Lowe, D., Masood, R., Rice, D. H., 2010. Biofilm detection with hematoxylin-eosin staining. Arch Otolaryngol Head Neck Surg 136(5):453-456.

[17] Xie, M. Y., Hou, L. J., Sun, J. J., Zeng, B., Xi, Q. Y., Luo, J. Y., et al., 2019. Porcine Milk Exosome MiRNAs Attenuate LPS-Induced Apoptosis through Inhibiting TLR4/NF-kappaB and p53 Pathways in Intestinal Epithelial Cells. J Agric Food Chem 67(34):9477-9491.

[18] Hou, L., Shi, J., Cao, L., Xu, G., Hu, C., Wang, C., 2017. Pig has no uncoupling protein 1. Biochem Biophys Res Commun 487(4):795-800.

[19] B, Lomenick, R, Hao, N, Jonai, RM, Chin, M, Aghajan, S, Warburton, et al., 2009. Target identification using drug affinity responsive target stability (DARTS). Proceedings of the National Academy of Sciences of the United States of America 106(51):21984-21989.

[20] S, Zhu, Z, Tian, D, Torigoe, J, Zhao, P, Xie, T, Sugizaki, et al., 2019. Aging- and obesity-related peri-muscular adipose tissue accelerates muscle atrophy. Plos One 14(8):e0221366.

[21] I, Alam, K, Lewis, JW, Stephens, JN, Baxter, 2007. Obesity, metabolic syndrome and sleep apnoea: all pro-inflammatory states. Obesity reviews : an official journal of the International Association for the Study of Obesity 8(2):119-127.

[22] H, Zhou, CJ, Urso, V, Jadeja, 2020. Saturated Fatty Acids in Obesity-Associated Inflammation. Journal of inflammation research 13:1-14.

[23] MY, Donath, SE, Shoelson, 2011. Type 2 diabetes as an inflammatory disease. Nature reviews. Immunology 11(2):98-107.

[24] RG, Baker, MS, Hayden, S, Ghosh, 2011. NF-κB, inflammation, and metabolic disease. Cell metabolism 13(1):11-22.

[25] P, Dandona, A, Aljada, A, Chaudhuri, P, Mohanty, R, Garg, 2005. Metabolic syndrome: a comprehensive perspective based on interactions between obesity, diabetes, and inflammation. Circulation 111(11):1448-1454.

[26] Herzig, S., Shaw, R. J., 2018. AMPK: guardian of metabolism and mitochondrial homeostasis. Nat Rev Mol Cell Biol 19(2):121-135.

[27] L, Shi, T, Zhang, Y, Zhou, X, Zeng, L, Ran, Q, Zhang, et al., 2015. Dihydromyricetin improves skeletal muscle insulin sensitivity by inducing autophagy via the AMPK-PGC-1α-Sirt3 signaling pathway. Endocrine 50(2):378-389.

[28] P, Sun, JB, Yin, LH, Liu, J, Guo, SH, Wang, CH, Qu, et al., 2019. Protective role of Dihydromyricetin in Alzheimer's disease rat model associated with activating AMPK/SIRT1 signaling pathway. Bioscience Reports 39(1).

[29] CJ, Green, M, Pedersen, BK, Pedersen, C, Scheele, 2011. Elevated NF-κB activation is conserved in human myocytes cultured from obese type 2 diabetic patients and attenuated by AMP-activated protein kinase. Diabetes 60(11):2810-2819.

[30] F, Yeung, JE, Hoberg, CS, Ramsey, MD, Keller, DR, Jones, RA, Frye, et al., 2004. Modulation of NF-kappaB-dependent transcription and cell survival by the SIRT1 deacetylase. The EMBO journal 23(12):2369-2380.

[31] J, Zhang, Y, Chen, H, Luo, L, Sun, M, Xu, J, Yu, et al., 2018. Recent Update on the Pharmacological Effects and Mechanisms of Dihydromyricetin. Frontiers in pharmacology 9:1204.

[32] F, Ciccarese, E, Zulato, S, Indraccolo, 2019. LKB1/AMPK Pathway and Drug Response in Cancer: A Therapeutic Perspective. Oxidative medicine and cellular longevity 2019:8730816.

[33] Kim, S., Yoon, Y. Y., Park, Y. W., Whang, W. K., Park, S. Y., Hwang, K. W., 2020. Cynandione A from Cynanchum wilfordii inhibits hepatic de novo lipogenesis by activating the LKB1/AMPK pathway in HepG2 cells. Journal of Natural Medicines 74(1):142-152.

[34] Tong, X., Smith, K. A., Pelling, J. C., 2012. Apigenin, a chemopreventive bioflavonoid, induces AMP-activated protein kinase activation in human keratinocytes. Molecular Carcinogenesis 51(3):268-279.

[35] Zhao, F., Huang, W. W., Zhang, Z., Mao, L., Han, Y. Y., Yan, J., et al., 2016. Triptolide induces protective autophagy through activation of the CaMKK beta-AMPK signaling pathway in prostate cancer cells. Oncotarget 7(5):5366-5382.

[36] Y, Zhao, Y, Zhou, M, Wang, 2019. Brosimone I, an isoprenoid-substituted flavonoid, induces cell cycle G phase arrest and apoptosis through ROS-dependent endoplasmic reticulum stress in HCT116 human colon cancer cells. Food & function 10(5):2729-2738.

[37] A, Gerbino, D, Russo, M, Colella, G, Procino, M, Svelto, L, Milella, et al., 2018. Dandelion Root Extract Induces Intracellular Ca Increases in HEK293 Cells. International Journal of Molecular Sciences 19(4).

[38] T, Murayama, N, Kurebayashi, 2019. Assays for Modulators of Ryanodine Receptor (RyR)/Ca Release Channel Activity for Drug Discovery for Skeletal Muscle and Heart Diseases. Current protocols in pharmacology 87(1):e71.

[39] A, McFedries, A, Schwaid, A, Saghatelian, 2013. Methods for the elucidation of protein-small molecule interactions. Chemistry & biology 20(5):667-673.

[40] MY, Pai, B, Lomenick, H, Hwang, R, Schiestl, W, McBride, JA, Loo, et al., 2015. Drug affinity responsive target stability (DARTS) for small-molecule target identification. Methods in molecular biology (Clifton, N.J.) 1263:287-298.

[41] B, Lomenick, G, Jung, JA, Wohlschlegel, J, Huang, 2011. Target identification using drug affinity responsive target stability (DARTS). Current protocols in chemical biology 3(4):163-180.

Figures

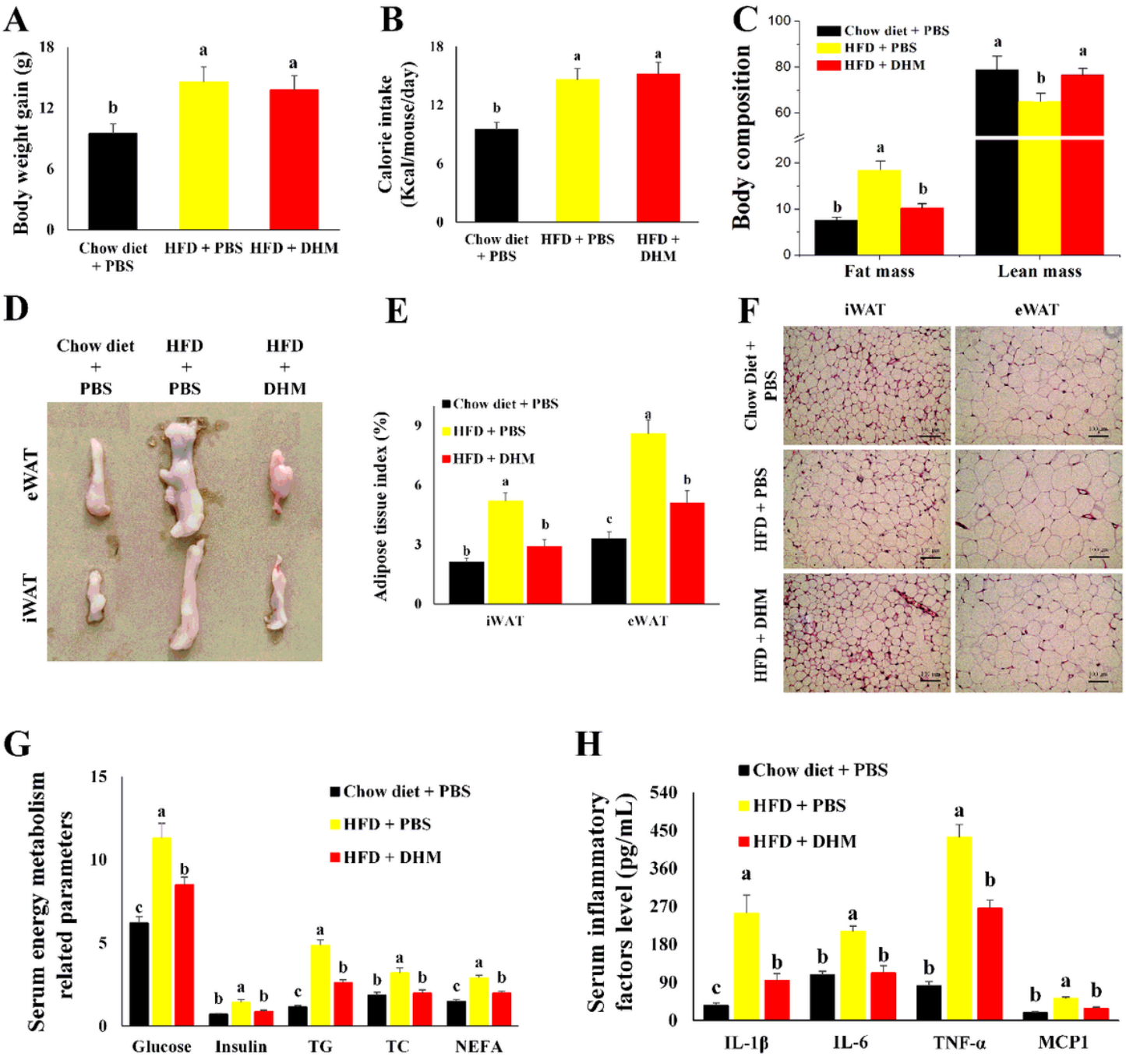

Figure 1

DHM reduced fat accumulation and inflammation in HFD-induced obese mice. A. DHM did not affect HFD-induced body weight gain in mice. B. DHM did not affect HFD-induced average daily energy intake. C. DHM prevented HFD-induced fat gain and muscle loss. D. Representative morphology image of mice adipose tissue. E. DHM inhibited HFD-induced adipose tissue hypertrophy, as shown by the percentage of adipose tissue index. F. HFD induced adipocytes hypertrophy, and DHM prevented HFD-induced adipocytes hypertrophy, as shown by H&E staining. G. DHM alleviated HFD-induced high levels of glucose, insulin, total triglycerides, total cholesterol, and free fatty acids in the serum. H. DHM reduced the increase of the HFD-induced inflammatory cytokines in serum. N = 6, * $p < 0.05$, ** $p < 0.01$, Bars with

different letters indicate they are significantly different (P<0.05). Magnification was 200×. The scale bar on the photomicrographs represents 100 μm.

Figure 2

DHM ameliorated inflammation-induced insulin resistance in HFD mice. A. HFD elevated the level of adipose tissue inflammatory cytokines in mice, and DHM suppressed the effect of HFD. B. Oral glucose tolerance test results showed that DHM improved HFD-induced insulin resistance C. HFD inhibited the mRNA level of AMPK, IRS-1, AKT, PI3K, and GLUT4. HFD increased the mRNA level of NF-κB and JNK. DHM reversed the mRNA level of inflammation-induced insulin resistance-related genes. D. HFD inhibited the protein level of p-AMPK, p-IRS-1, p-AKT, p-PI3K, and GLUT4. HFD increased the protein level of p-NF-κB and JNK. DHM reversed the protein level of inflammation-induced insulin resistance-related genes. “p-” before the gene name means phosphorylated form. N = 6, Bars with different letters indicate they are significantly different (P<0.05).

Figure 3

TNFα induced inflammatory response and insulin resistance in 3T3-L1 cells. A. The optimal TNFα concentration used in 3T3-L1 experiments was determined by MTT. B. The glucose uptake test confirmed that TNFα induced insulin resistance in 3T3-L1 cells. C. Quantitative analysis of fluorescence intensity in Figure 3B using Image J software. D. mRNA level of inflammation-induced insulin resistance-related genes was determined by qPCR. E. The protein level of inflammation-induced insulin resistance-related genes was measured by WB. “p-” before the gene name means phosphorylated form. F. N = 6, * p < 0.05, ** p < 0.01, Bars with different letters indicate they are significantly different (P<0.05). Magnification was 100×. The scale bar on the photomicrographs represents 50 μm.

Figure 4

DHM ameliorated the inflammatory-induced insulin resistance. A. The optimal DHM concentration used in 3T3-L1 was determined by MTT. B. The glucose uptake test confirmed that TNFα induced insulin resistance in 3T3-L1 cells. C. Quantitative analysis of fluorescence intensity in Figure 4B using Image J software. D. The effect of DHM on the mRNA level of the inflammatory-induced insulin resistance-related genes was measured by qPCR. E. The effect of DHM on the protein level of the inflammatory-induced insulin resistance-related genes was detected by WB. “p-” before the gene name means phosphorylated form. N = 6. Bars with different letters indicate they are significantly different (P<0.05). Magnification was 100×. The scale bar on the photomicrographs represents 50 μm.

Figure 5

DHM ameliorated inflammation-induced insulin resistance through AMPK. A. DHM alleviated TNFα-induced insulin resistance was dependent on AMPK, as shown by the glucose uptake test. B. Quantitative analysis of fluorescence intensity in Figure 5A using Image J software. C. DHM regulated the mRNA level of inflammatory response-induced insulin resistance-related genes was dependent on AMPK, as shown by qPCR. D. DHM regulated the protein level of inflammatory response-induced insulin resistance-related genes was dependent on AMPK, as shown by WB. N = 6. Bars with different letters indicate they are significantly different ($P<0.05$). Magnification was 100×. The scale bar on the photomicrographs represents 50 μm.

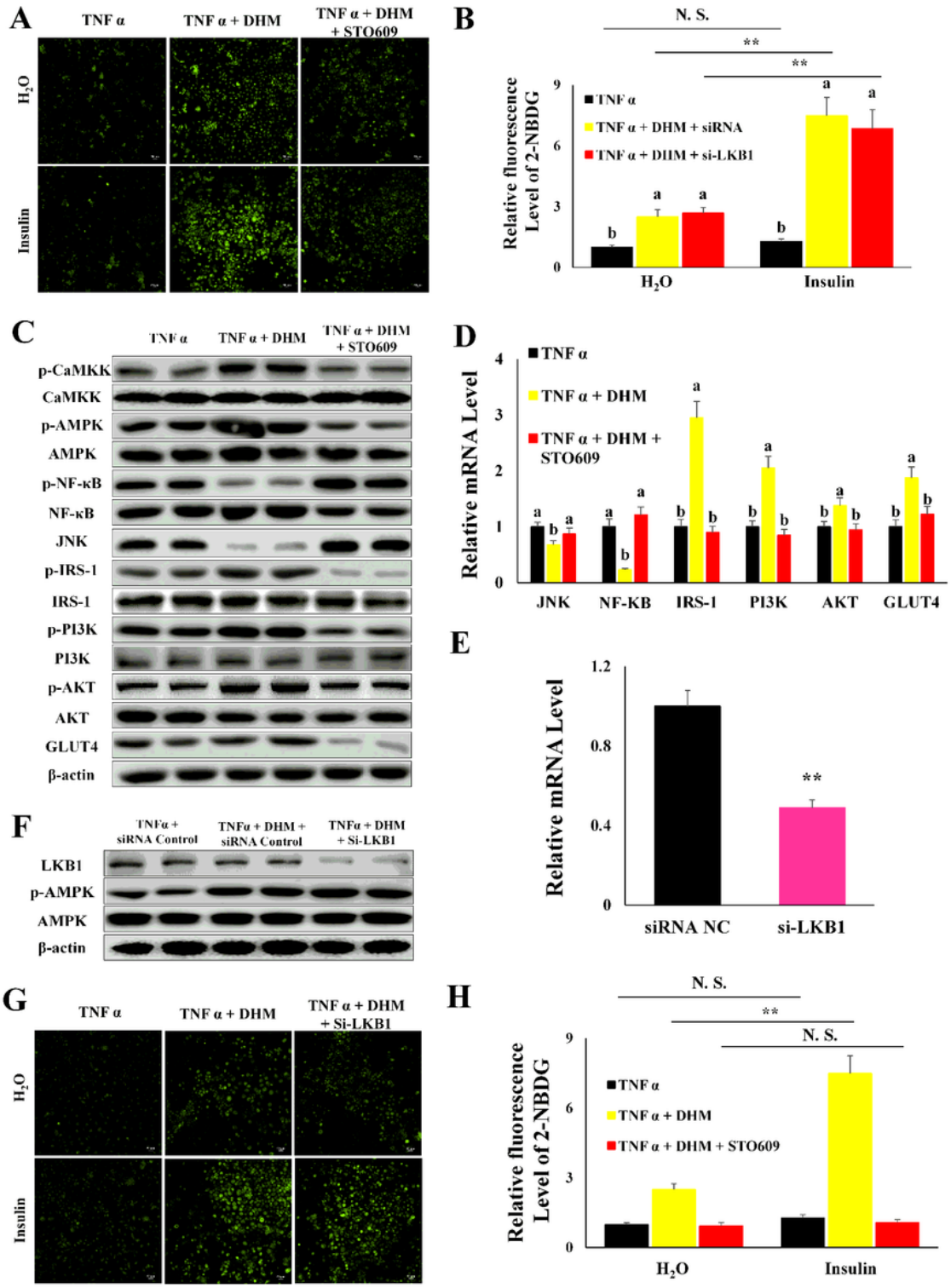

Figure 6

DHM ameliorated inflammation-induced insulin resistance through CaMKK-AMPK instead of the LKB1-AMPK pathway. A. DHM alleviated TNFα-induced insulin resistance was dependent on CaMKK, as shown by the glucose uptake test. B. Quantitative analysis of fluorescence intensity in Figure 6A using Image J software. C. DHM regulated the protein level of inflammatory response-induced insulin resistance-related genes was dependent on CaMKK, as shown by WB. “p-” before the gene name means phosphorylated

form. D. DHM regulated the mRNA level of inflammatory response-induced insulin resistance-related genes was dependent on CaMKK, as shown by qPCR. E. LKB1 was interfered with by small RNA, as shown by qPCR. F. LKB1 interference did not affect the AMPK expression, as shown by WB. “p-” before the gene name means phosphorylated form. G. LKB1 did not affect DHM improvement on TNFα-induced insulin resistance, as shown by the glucose uptake test. H. Quantitative analysis of fluorescence intensity in Figure 6G using Image J software. N = 6, ** p <0.01. Bars with different letters indicate they are significantly different (P<0.05). Magnification was 100×. The scale bar on the photomicrographs represents 50 μm.

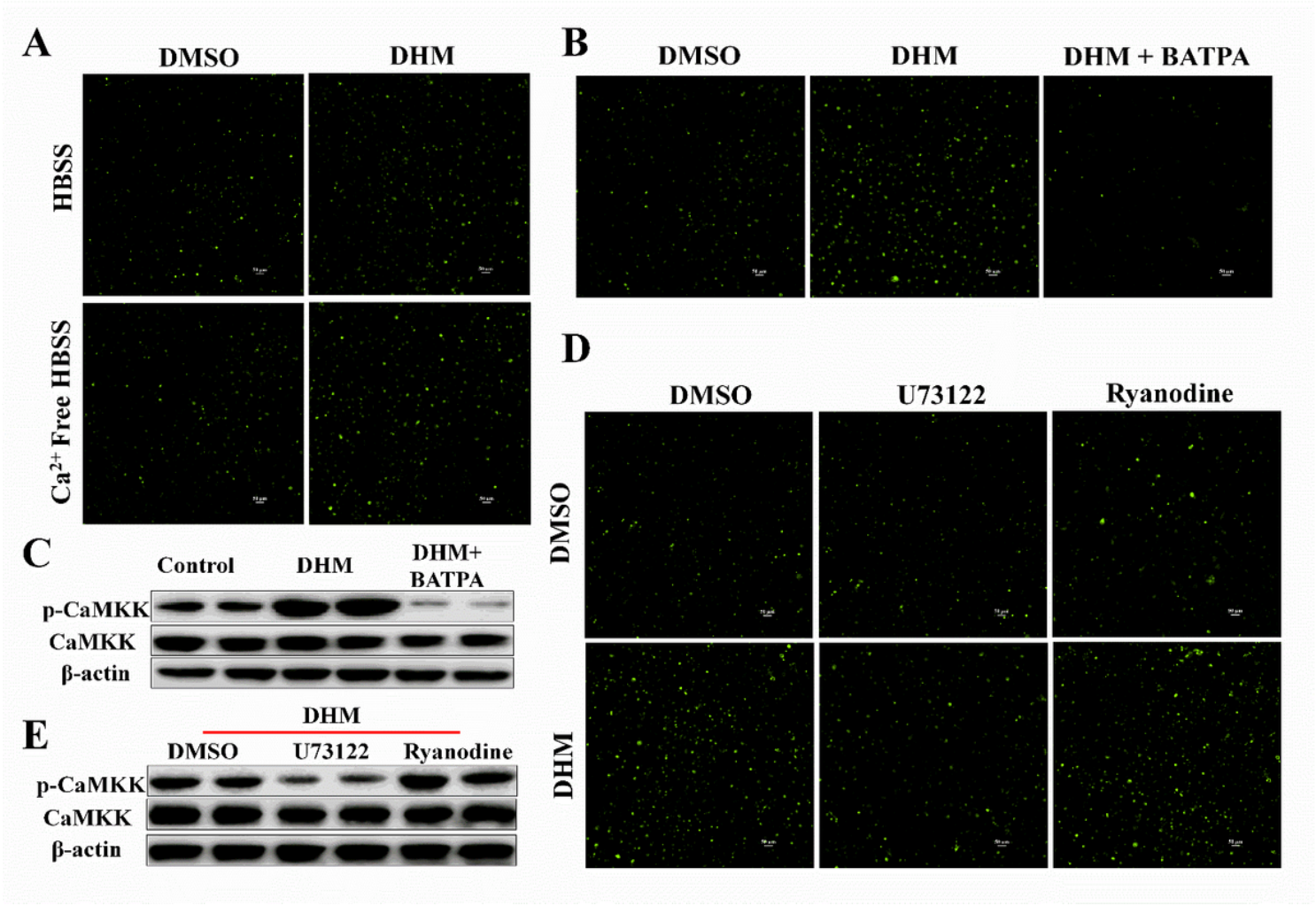

Figure 7

DHM activated CaMKK by increasing intracellular Ca2+ concentration through the PLC-IP3 receptor pathway. A. DHM increased intracellular Ca2+ signal, as shown by the Ca2+ probe test. B. After cellular Ca2+ was cleared, the activation effect of DHM on intracellular Ca2+ was eliminated, as shown by the Ca2+ probe test. C. The effect of DHM on CaMKK activation depended on intracellular Ca2+ signal, as shown by WB. D. DHM increased intracellular Ca2+ concentration was dependent on the PLC-IP3 receptor pathway, as shown by the Ca2+ probe test. E. The effect of DHM on CaMKK activation depended on the intracellular PLC-IP3 receptor pathway, as shown by WB. N = 6.

Figure 8

DHM ameliorated inflammatory-induced insulin resistance through interaction with PLC. A. DHM might interact with the PLC, as shown by DARTS, lines 1 to 5 represent molecular weight marker, DMSO, 10 nM DHM, and 1 μM DHM, respectively. B. DHM promoted the stability of PLC protein, as shown by WB. C. The effect of DHM on the mRNA level of inflammatory response-induced insulin resistance-related genes was dependent on the PLC-IP3 receptor pathway, as shown by qPCR. D. The effect of DHM on the protein level of inflammatory response-induced insulin resistance-related genes was dependent on the PLC-IP3 receptor pathway, as shown by WB. “p-” before the gene name means phosphorylated form. E. DHM alleviated TNFα-induced insulin resistance was dependent on the PLC-IP3 receptor pathway, as shown by the glucose uptake test. F. Quantitative analysis of fluorescence intensity in Figure 8E using Image J software. N = 6. Bars with different letters indicate they are significantly different ($P<0.05$). Magnification was 100×. The scale bar on the photomicrographs represents 50 μm.

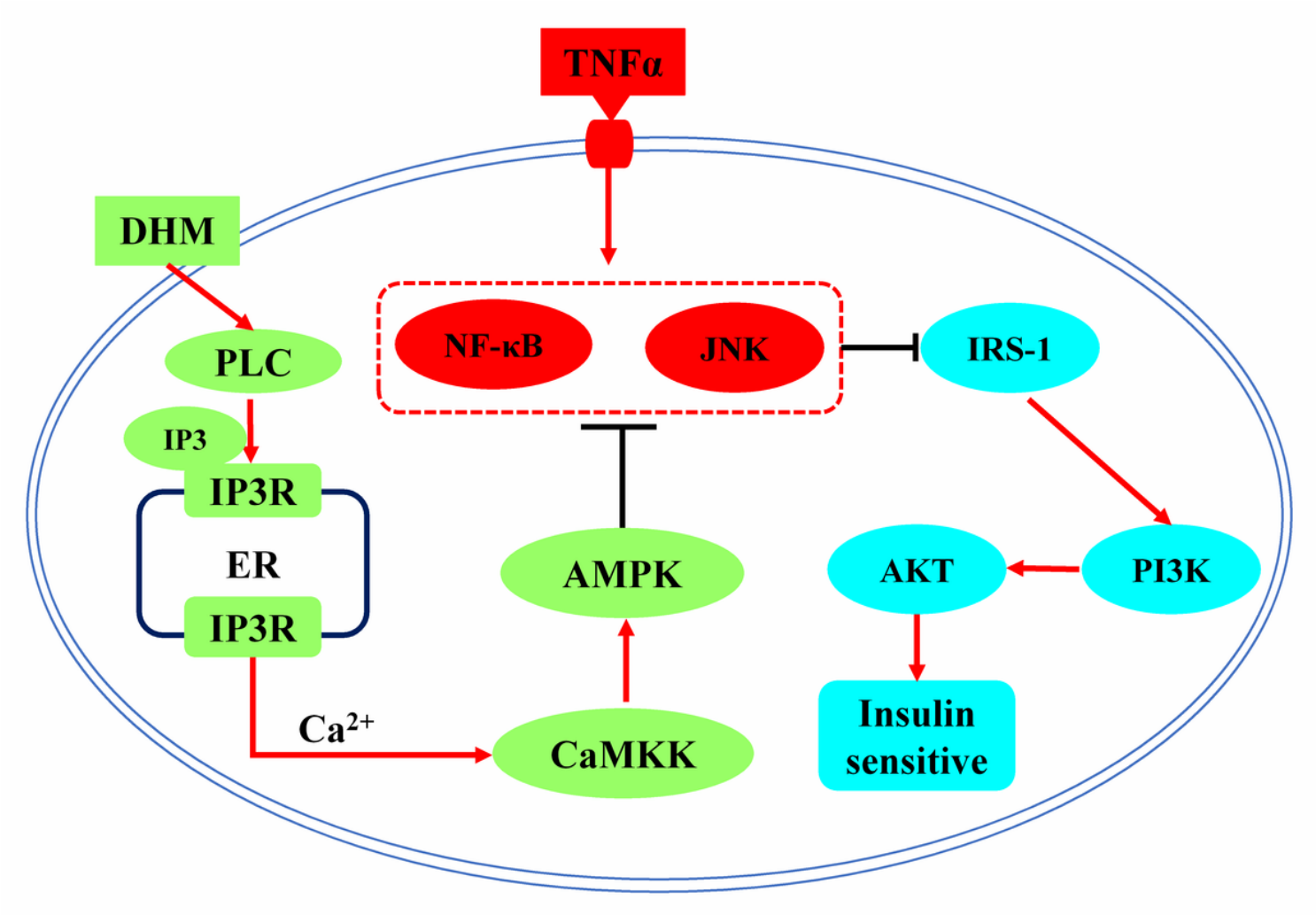

Figure 9

Summary model of DHM improves inflammation-induced insulin resistance via phospholipase C-CaMKK-AMPK signal pathway